Actor's and observer's primary motor cortices stabilize similarly after seen or heard motor actions

Gina Caetano*, Veikko Jousmäki*, and Riitta Hari*†‡

*Brain Research Unit, Low Temperature Laboratory, Helsinki University of Technology, P.O. Box 2200, FIN-02015 HUT, Espoo, Finland; and †Department of Clinical Neurophysiology, Helsinki University Central Hospital, FIN-00290, Helsinki, Finland

Contributed by Riitta Hari, March 15, 2007 (sent for review July 3, 2006)

We quantified rhythmic brain activity, recorded with whole-scalp magnetoencephalography (MEG), of 13 healthy subjects who were performing, seeing, or hearing the tapping of a drum membrane with the right index finger. In the actor's primary motor (M1) cortex, the level of the ≈20-Hz brain rhythms started to decrease, as a sign of M1 activation, ≈2 s before the action and then increased, with a clear rebound ≈0.6 s after the tapping, as a sign of M1 stabilization. A very similar time course occurred in the M1 cortex of the observer: the activation, although less vigorous than in the actor, started ≈0.8 s before the action and was followed by a rebound. When the subject just heard the tapping sound, no preaction activation was visible, but a rebound followed the sound. The ≈10-Hz somatosensory rhythm, which also started to decrease before own and viewed actions, returned to the baseline level ≈0.6 s later after own actions than observed actions. This delay likely reflects proprioceptive input to the cortex, available only during own actions, and therefore could be related to the brain signature of the sense of agency. The strikingly similar motor cortex reactivity during the first and third person actions expands previous data on brain mechanisms of intersubjective understanding. Besides motor cortex activation before own and observed (predicted) actions, the M1 cortex of both the viewer and the listener stabilized in a very similar manner after brisk motor actions.

brain rhythms | intersubjectivity | magnetoencephalography | mirror neurons | motor cortex

A large part of our social interaction is based on nonverbal communication that relies on facial expressions, gaze, postures, and gestures, all used to interpret other people's intentions, motivations, and feelings.

A very important contribution to the understanding of the neural basis of human nonverbal communication came from the identification and characterization of an action observation/execution matching system in monkey frontal-lobe area F5 (1, 2). A similar action/observation matching network, the mirror-neuron system (MNS), has been identified in the human brain by neuroimaging studies (for a review, see ref. 3). Experiments carried out while the subjects observed actions performed by others indicate that the human MNS includes at least the inferior frontal gyrus (Broca's region and its right hemisphere homologue, the human counterparts of the monkey F5 area) and the primary motor (M1) cortex in the precentral cortex. Moreover, the motor mirror neurons receive contribution from the superior temporal sulcus via the inferior parietal lobule (4–9). In the monkey brain, the inferior parietal lobule also contains mirror neurons, which are supposed to contribute to the understanding of the actor's intentions (10).

Anatomically, the M1 cortex is downstream from the inferior frontal gyrus (IFG), the core area of the MNS, and therefore the reactivity of the IFG can be reflected in the functional state of the M1 cortex. The human M1 cortex is activated both during observation and execution of motor tasks, as has been demonstrated by monitoring the ≈20-Hz oscillatory activity of the M1 cortex with magnetoencephalography (MEG) (6).

The motor cortex ≈20-Hz activity is a part of the Rolandic μ rhythm; the other, ≈10-Hz component receives a strong contribution from the primary somatosensory (S1) cortex (11, 12). Both components are suppressed during brisk movements, whereas their level increases after the movement, a phenomenon known as a "rebound."

Several findings relate the ≈20-Hz postmovement rebound to stabilization of the motor cortex after any perturbation: first, the rebound occurs after both voluntary finger movements and after passive movements elicited by electric median nerve stimuli (11). Second, the motor cortex excitability, probed with transcranial magnetic stimulation, is reduced during the 20-Hz rebounds (13). Third, the ≈20-Hz level increases during immobility (14) and after administration of GABAergic benzodiazepine (15). Fourth, during isometric contraction, the ≈20-Hz oscillations are coherent with surface electromyogram (EMG). This cortex–muscle coherence is typically reduced or abolished in the beginning of a movement, whereas it is prominent during static phases of motor tasks, increasing immediately after the end of a phasic movement, provided that the steady contraction is still maintained (16). Intraoperative cortical stimulation in patients in whom the cortical site of the cortex–muscle coherence was preoperatively determined (17), as well as combined transcranial magnetic stimulation and cortex–muscle coherence studies, in patients with congenital hemiparesis (18), further indicate that the Rolandic ≈20-Hz oscillations mainly originate from the M1 cortex. Thus, the ≈20-Hz rebound likely arises from the motor cortex, being related to increased cortical inhibition and thereby to stabilization of the M1 cortex.

In the present study, we probed the functional state of the sensorimotor cortex by monitoring oscillatory MEG activity. The aim was to find possible similarities between own motor action vs. visual and auditory observation of other person's similar actions. Action-related sounds were included because the monkey mirror neurons also react to sounds of hand actions (19) and because many human actions are easily recognized from the associated sounds, even when the actor is invisible. In humans, action-related sounds have been shown to change the corticospinal excitability (20).

Previous studies have demonstrated important similarities between the first and third person before and during motor actions, both in behavior and in motor cortex reactivity. First,

Author contributions: G.C., V.J., and R.H. designed research; G.C. performed research; V.J. contributed new nonmagnetic drum tools; G.C. and R.H. analyzed data; and G.C., V.J., and R.H. wrote the paper.

The authors declare no conflict of interest.

Freely available online through the PNAS open access option.

Abbreviations: MNS, mirror-neuron system; MEG, magnetoencephalography; EMG, electromyogram; TFR, time-frequency representation; S1, primary somatosensory; M1, primary motor.

See Commentary on page 8683.

‡To whom correspondence should be addressed. E-mail: hari@neuro.hut.fi.

This article contains supporting information online at www.pnas.org/cgi/content/full/0702453104/DC1.

www.pnas.org/cgi/doi/10.1073/pnas.0702453104

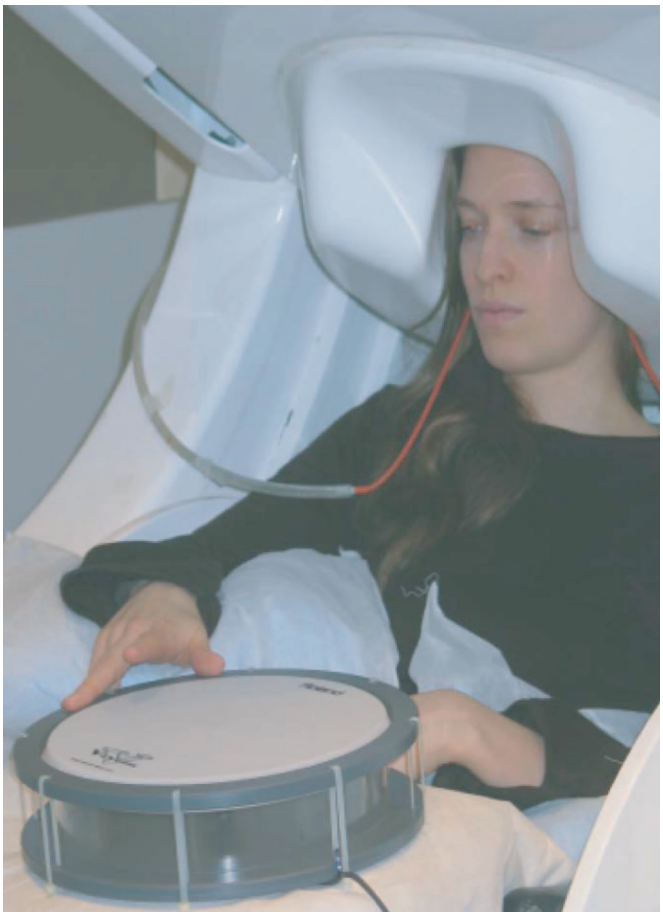

Fig. 1. Experimental setup. The subject, sitting with her head supported by the helmet-shaped neuromagnetometer, is tapping the nonmagnetic drum with her right index finger while looking at her hand.

during attentive observation of well-predictable hand movements, the eye fixations of the viewer precede locations of the actor's hand, slightly later but otherwise similarly as the fixations of the actor (21). Second, premovement electroencephalographic activation in the viewer's brain (although weaker) is similar to that in the actor's brain (22). Third, the motor cortex is activated during manipulative finger movements similarly (although less intensively) in the actor and in the viewer (6).

Here we expand the similarities of brain mechanisms between the viewer and actor to the whole action sequence by showing that the M1 cortex, besides activating before own and observed actions, stabilizes after the movements in a highly similar manner both in the actor's and observer's brain.

Results

We quantified cortical MEG signals recorded from 13 subjects (preselected among 25 on the basis of clear cortical reactivity; see *Methods* and supporting information (SI) Fig. 5). The subjects (*i*) rested relaxed, (*ii*) tapped a drum membrane (see Fig. 1) once every 3–6 s with their right index finger (*Own Action*), (*iii*) tapped the drum without hearing the sound due to continuous auditory masking with white noise (*Own Action No Sound*), (*iv*) observed another person tapping the drum once every 4–5 s (*Observation*), and (*v*) listened to another person tapping the drum without seeing the action (*Drum Sound*).

Fig. 2 *Left* shows, for a representative subject, that the level of the ≈20-Hz oscillations increased within 1 s after each *Own Action*; the times of actions are visible as EMG bursts. During

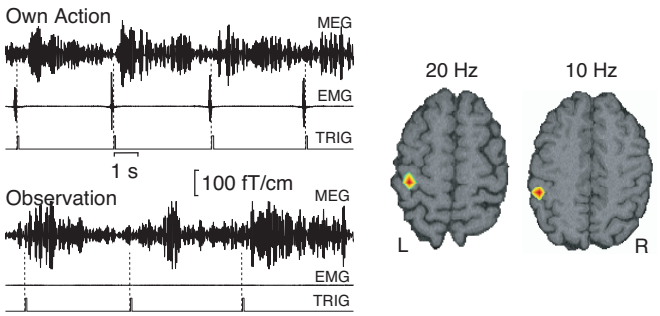

Fig. 2. Reactivity of the MEG signals and source locations of the ≈20-Hz oscillations in a single subject. (*Left*) MEG signals bandpass-filtered through 14–28 Hz (in this subject) during *Own Action* and *Observation* conditions from a representative channel over the left motor cortex, the EMG from the (right) first interosseus muscle, and the trigger (TRIG) from the drum. (*Right*) Density plot of the current dipoles for the ≈20-Hz (n = 48) and ≈10-Hz (n = 52) oscillations; red refers to the highest density. The respective Talairach coordinates of the clusters' centers agree with the location of the M1 cortex (−34, −19, 57) and of the S1 cortex (−46, −26, 46) (Talairach Daemon Client version 2.0; http://ric.uthscsa.edu/resources).

Observation, similar rebounds of the ≈20-Hz oscillations followed each finger tap of the other person, although the subject's own EMG was silent.

The source clusters of the ≈20- and ≈10-Hz oscillations, superimposed on the subject's brain in Fig. 2 *Right*, indicated, in agreement with previous findings (11, 12), that the ≈20-Hz oscillations mainly arise from the precentral M1 cortex and that the ≈10-Hz oscillations mainly arise from the slightly more posterior S1 cortex.

Fig. 3 shows the mean ± SEM levels of the ≈20- and ≈10-Hz oscillations of the 13 subjects selected (see *Methods*) during *Own Action*, *Own Action No Sound*, *Observation*, and *Drum Sound* conditions. The ≈20-Hz activity starts to decrease at −2 s during *Own Action* and *Own Action No Sound* conditions and at −0.8 s during *Observation*. The maximum suppression is seen ≈150 ms

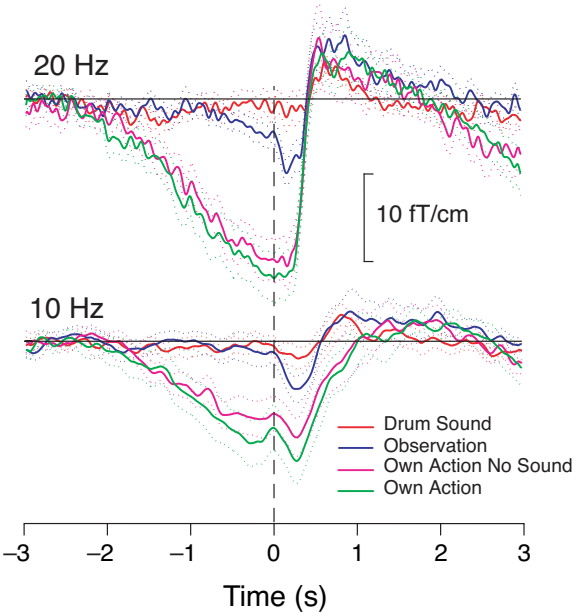

Fig. 3. Mean ± SEM level (solid and dotted lines, respectively) across 13 subjects of the ≈20- and ≈10-Hz oscillations during *Own Action* (with sound), *Own Action No Sound*, *Observation*, and *Drum Sound*. Baseline is from −2.9 s to −2.4 s.

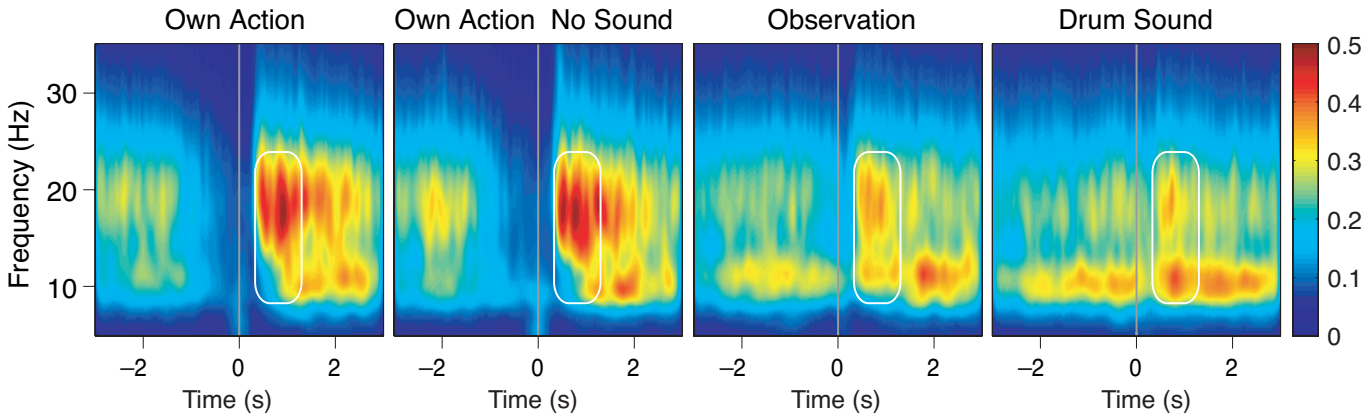

Fig. 4. Average TFRs across 13 subjects during *Own Action*, *Own Action No Sound*, *Observation*, and *Drum Sound* conditions. The TFRs are shown for intervals from −3 to 3 s and for frequencies from 5 to 35 Hz; the color bar indicates the amplitude scale $(fT/cm)^2$.

after the tap, and it is followed by a rebound that peaks at ≈600 ms. A similar pattern is observed for ≈10-Hz activity, with the maximum suppression at ≈270 ms after the tap, in all four conditions, followed by a tiny rebound that peaks ≈600 ms later for own actions than observed actions.

During the *Observation* condition, the maximum suppression of the 20-Hz activity was only 42 ± 9% of that during *Own Action* ($P < 0.005$, two-tailed paired t test, $n = 13$). The ≈20-Hz rebounds, measured as the mean values from 500 to 900 ms, were, in all four conditions, statistically significantly ($P < 0.05$) above the baseline (defined as the mean level from −2.9 to −2.4 s), without any systematic differences in the peak amplitudes. Nor did the latencies of the maximum suppression, of the rebound onset, or of the rebound peak differ between the conditions.

When the rebounds were computed with respect to a baseline from −600 to 0 ms (during the suppression period before the tap), the ≈20-Hz level crossed the baseline 178 ± 5 ms later ($P < 0.0005$, $n = 13$) during the *Observation* than during the *Own Action* condition. Thus, the selection of a baseline too close to the action would result in a rather different picture of the relative timings of the rebounds in different conditions.

For the ≈10-Hz oscillations, only tiny rebounds were visible, but they were not statistically significant with respect to the baseline from −2.9 to −2.4 s. The maximum suppression occurred at about the same time for all conditions, but during *Observation*, the suppression was only 46 ± 16% ($P < 0.05$) of that observed during *Own Action*. Strikingly, the ≈10-Hz level returned to the baseline 580 ± 195 ms ($P < 0.05$, $n = 10$) later during *Own Action* than during *Observation*.

Further examination of the *Own Action* traces in Fig. 3 shows approximately similar onset times and durations for the ≈20-Hz and ≈10-Hz suppressions but a statistically significantly slower recovery for the ≈10-Hz than for the ≈20-Hz activity (slopes from the maximum suppression to the peak rebound were 24 ± 5 $fT \cdot cm^{-1} \cdot s^{-1}$ and 69 ± 12 $fT \cdot cm^{-1} \cdot s^{-1}$, respectively; $P < 0.005$).

In the original group of all 25 subjects, the averaged signals were similar, with statistically significant ≈20-Hz rebounds in all conditions, but the mean rebound amplitudes were weaker (by 40–50% during own and observed actions, measured from maximum suppression to maximum rebound), and the intersubject variability was larger than in the study group of 13 persons.

Additional control recordings in three subjects showed no ≈20-Hz rebounds to 1-kHz tone pips presented once every 4 s.

The time-frequency representations (TFRs) for the four conditions across the 13 subjects (Fig. 4) demonstrate a picture very similar to the above temporal spectral evolution analysis: clear ≈20-Hz rebounds after *Own Action* and *Own Action No Sound* and weaker rebounds after *Observation* and *Drum Sound*. Similar intensity differences are also evident in the ≈10-Hz band. During *Own Action* and *Own Action No Sound*, the ≈10-Hz level returns back to baseline clearly later than the ≈20-Hz level. In contrast, after *Observation* and *Drum Sound*, the rebounds start at approximately the same time in both frequency bands.

Reactivity of both ≈20- and 10-Hz rhythms was observed in both contra- or ipsilateral hemispheres. Although the spatial patterns were similar in the *Own Action*, *Observation*, and *Drum Sound* conditions, reflecting modulations in about the same brain regions, the relative timing of the signals varied to some extent in the two hemispheres (see SI Fig. 6 *a* and *b*).

Discussion

Our findings on the ≈20-Hz and ≈10-Hz reactivity indicate that both the M1 and S1 cortices, the main generator areas of these brain rhythms, were activated during both own action and action observation conditions, in full agreement with previous findings (6, 11). The postmovement ≈20-Hz rebound, well known to follow own actions, has been previously observed with EEG in the viewer's brain (23). We now show that such a rebound occurs after both seen and heard motor actions at about the same time that it occurs after self-performed actions, strongly supporting stabilization of the motor cortex in the viewer's brain after the observed action has ended.

We also showed that suppression of the ≈20-Hz activity starts before both own and observed actions, although much earlier for self-performed actions; the result supports predictive activation of the M1 cortex in the viewer's brain during observed actions. Our finding, however, differs from the results of Kilner *et al.* (22), who showed that the slow premovement EEG shifts ("Bereitschaftpotentials") start at the same time for both own and observed actions. However, in contrast to our experimental setup, the observed movements in their study were totally predictable once the cue (a colored light to encode the movement vs. no movement) had been presented.

Neural Underpinnings of Intersubjectivity and the Sense of Agency. Differences between the first and third person's perspectives have been discussed extensively in both philosophy (e.g., ref. 24) and in social psychology (e.g., ref. 25). Interestingly, the rapid progress in human neuroimaging is providing new clues about the underlying brain mechanisms. Although the mental states are private, humans can obtain information about other persons' feelings and intentions through verbal and nonverbal communication. Phenomenological philosophers often consider the body as the display site of the mind, meaning that we can read

some aspects of others' mental contents by reacting to and interpreting bodily expressions.

The MNS has been suggested to form the basis of understanding other people's motor actions (3). Within this framework, other people's actions are considered to trigger in the observer internal simulation of similar actions and thereby even prediction of other people's goal-directed movements. A central role in this process is taken by the core part of the human MNS, the inferior frontal gyrus and its reciprocal connections with the parietal lobe; these connections seem dysfunctional in high-functioning autistic subjects suffering from Asperger's syndrome (26).

The activation of the observer's own motor system leads to a problem of distinguishing between self and others at the neuronal level. Proposed solutions include at least efference copies from the movement preparation areas and proprioceptive input during own movements, as well as weaker activation of the motor system during observed than during performed action (for reviews, see refs. 27 and 28).

Several brain areas contribute to the sense of agency: the inferior parietal lobe, the precuneus, and the somatosensory cortex (29), as well as the superior parietal lobule, an integration area of visual and somatosensory inputs to motor outputs (30). Moreover, important areas, in terms of self-reference, exist in the mesial cortical areas (31) and in the somatosensory cortex (32).

Our data give additional support for the role of somatosensory afference in distinguishing self and others at the neuronal level. The ≈10-Hz activity recovered to the baseline level ≈580 ms later during *Own Action* than during *Observation*. This delay could reflect the more intensive and longer effect on the S1 cortex by the afferent somatosensory input during *Own Action* than by the neuronal activity related to the simulated motor actions seen in others during *Observation*.

Previous studies have indicated that the S1 activity can be modulated by imagined and observed movements (33–35). One possible route for the S1 activation and the related ≈10-Hz suppression, besides direct somatosensory input, is via reciprocal cortical connections between the pre- and postcentral cortices during both motor action and motor imagery.

The observed delay of the ≈10-Hz recovery during *Own Action* could thus be a cortical-level correlate for the sense of agency, indicating that the somatosensory cortical network has a plausible role in the internal simulation of the sensory consequences of other person's movements, either seen or heard. The presence vs. absence of proprioceptive feedback helps to maintain a sound sense of agency.

Conclusion

Our results demonstrate that the similarities in neural mechanisms between the actor's and the viewer's brains extend beyond the motor cortex activation before and during the movement to the postmovement stabilization of the motor cortex after the seen or heard action. Furthermore, the somatosensory cortex plausibly plays an important role in the internal simulation of the observed action by contributing to the distinction between own and other's actions on the basis of sensory and proprioceptive feedback. The unraveled motor and sensory mechanisms further emphasize and extend the qualitative similarities between the first and third person's brain mechanisms and likely support intersubjective understanding between interacting persons.

Materials and Methods

Subjects. We screened 25 healthy adults with no history of neurological nor hearing disorders but selected for further analysis only those 13 subjects (29.5 ± 4.5 yrs; six females and seven males; all right-handed) who showed a clear reactivity in their brain rhythms, i.e., at least a 10 fT/cm increase in the motor cortex ≈20-Hz level after *Own Action* ("rebound," mean values from 500 to 900 ms with respect to the time of drum tapping, with a baseline from −600 to 0 ms; see SI Fig. 5). An informed consent was obtained from all subjects after explanation of the experiment. The MEG recordings had a prior approval by the local ethics committee.

Experimental Setup and Stimuli. A silent electronic Roland V-drum (Roland, Hamamatsu, Shizuoka, Japan) was adapted to be totally nonmagnetic. The signal from the drum's piezoelectric transducer was used both to produce a trigger for MEG signal averaging and to obtain the action-sound from tapping the drum membrane. The sounds were presented through plastic tubes to ear pieces (Etymotic Research Inc., Elk Grove Village, IL) tightly fitted into the ear canals. The loudness of the tapping sound was ≈66 dB sound pressure level, and the loudness of the white noise used for auditory masking was 69 dB, and both were kept constant for all subjects.

Control sounds, 100-ms tone bursts (1 kHz, 80-ms plateau and 10-ms rise and fall time; ≈74 dB) were presented binaurally once every 4 s to three of the subjects participating in the main study.

The experimenter sat on a bench on the right side of the subject at a right angle with respect to the subject's heading direction and sitting position. The subject was able to see only the right forearm of the experimenter, who stayed behind a white screen of paper. During both *Observation* and *Drum Sound* conditions, the experimenter tapped the drum briskly with his right index finger.

The subjects trained the brisk tapping movement with time intervals of ≈4 s (without counting) before entering the measurement room and when in position to be measured. However, during the experiment, the individual tapping intervals varied from 3 to 6 s. For the experimenter, who was allowed to count silently the intervals, the intervals varied from 4 to 5 s.

MEG Recordings. Cortical MEG signals were recorded with a 306-channel neuromagnetometer (Vectorview; Neuromag Ltd., Helsinki, Finland) that houses 102 identical triple-sensor elements in a helmet-shaped array. Each sensor element consists of two orthogonal planar gradiometers and one magnetometer, providing three independent measurements of the magnetic field. The planar gradiometers measure the two orthogonal tangential derivatives of the magnetic field component that is normal to the helmet surface at the sensor location, and they detect the largest signal just above a local dipolar current source (36).

During the MEG recording, the subjects were sitting comfortably in a magnetically shielded room, with their head tightly pressed against the helmet-shaped neuromagnetometer. They were asked to keep their head immobile and their eyes open and to avoid eye blinking during the stimulation.

MEG signals were recorded with a 0.03–172 Hz passband and were digitized at 600 Hz. Surface EMG was recorded from the extensor indicis proprius muscle in the right forearm in all subjects, and also from the right first interosseous muscle in three subjects. Two sets of 35 single trials were averaged online to check replicability during the *Own Action*, *Own Action No Sound*, *Observation*, and *Drum Sound* conditions; 100 single trials were averaged in the *Control* condition. The analysis epochs lasted for 3,500 ms, including a prestimulus baseline of 1,000 ms. Vertical and horizontal electrooculograms (EOGs) were measured simultaneously, and epochs coinciding with EOG signals exceeding 300 μV were rejected from the MEG analysis. Spontaneous activity was recorded continuously so that 70–150 (mean across subjects = 91) single trials, each containing one action, were collected; the data were stored on a magnetooptical disk for offline analysis.

Four head position indicator coils were attached to the subject's scalp to measure the head position with respect to the sensor array. The locations of these coils were determined with respect to three anatomical landmarks (left and right preauric-

ular points and nasion) by using a 3D digitizer (Isotrak 3S10002; Polhemus Navigation Sciences, Colchester, VT). The magnetic fields generated by currents fed into the head position indicator coils were then measured when the subject was in the position for the experiment, and the locations of the coils were determined with respect to the sensor array. The anatomical landmarks and additional points were used to align MEG and magnetic resonance image coordinate systems. The structural magnetic resonance images of the subject's brain were acquired by using a 1.5-T Siemens Magnetom system (Siemens, Erlangen, Germany).

Data Analysis. Stimulus-related changes in the level of the ≈10-Hz and ≈20-Hz sensorimotor oscillations were visualized by calculating temporal spectral evolution and TFRs for epochs starting 3 s before and ending 3 s after the trigger pulses that indicated the times of the tappings.

Temporal spectral evolution. The level of the oscillatory activity was quantified from traces obtained by first bandpass filtering the signals through 8–13 Hz for the ≈10-Hz band and through 14–30 Hz, depending on the individual frequency maxima, for the ≈20-Hz band. The filtered signals were then rectified and finally averaged time-locked to the stimuli (11). We included all epochs because, for example, eye-blink artifacts are in a different frequency range than the frequency bands of interest. The strengths of the ≈10-Hz and ≈20-Hz rebounds were determined, for each subject, from the MEG channel over the left Rolandic cortex that showed the strongest ≈20-Hz reactivity during *Own Action*. The mean ± SEM across subjects was calculated for both the 13 selected subjects (presented in Fig. 3 and discussed throughout the article) and for the full set of 25 subjects, with respect to baseline from −2.9 s to −2.4 s.

TFR. The TFRs were calculated from the channel selected for the analysis of the temporal spectral evolution in each subject. Frequencies of 5–35 Hz, with steps of 0.25 Hz, were analyzed by using wavelets with a width of seven cycles. A grand-average TFR was calculated separately, across the 13 selected subjects, for all four experimental conditions.

Source modeling. For source identification, the head was modeled as a spherical conductor, with the origin defined from the individual magnetic resonance images (36). Equivalent current dipoles (ECDs) were found by least-squares fits of signals obtained in the *Own Action* condition, both for ≈20-Hz oscillations and for ≈10-Hz oscillations occurring 0.5–2.0 s after the tap. The sources were identified on the basis of 18 sensors over the left Rolandic area, where the signals were the largest. Only ECDs with goodness of fit (g) exceeding 80% were accepted. The spatial density was computed for 48 and 52 source locations, respectively, and superimposed on the individual magnetic resonance images.

We thank Helge Kainulainen for technical help in modifying the drum; Jan Kujala (Helsinki University of Technology) for providing the software for source density plots; and Henri Autti, Jari Kainulainen, Seppo Mattila, and Sini Salonen for assistance in running the experiments. This work was supported by the Academy of Finland (National Centers of Excellence Program 2006–2011), the Sigrid Jusélius Foundation in Finland, the Instrumentarium Foundation in Finland, and Fundação para a Ciência e Tecnologia Programa Praxis XXI BD-6206/2001 in Portugal.

1. Gallese V, Fadiga L, Fogassi L, Rizzolatti G (1996) *Brain* 119:593–609.
2. Rizzolatti G, Fadiga L, Gallese V, Fogassi L (1996) *Cogn Brain Res* 3:131–141.
3. Rizzolatti G, Craighero L (2004) *Annu Rev Neurosci* 27:169–192.
4. Fadiga L, Fogassi L, Pavesi G, Rizzolatti G (1995) *Eur J Neurosci* 11:3983–3994.
5. Rizzolatti G, Fadiga L, Matelli M, Bettinardi V, Paulesu E, Perani D, Fazio F (1996) *Brain Res* 111:246–252.
6. Hari R, Forss N, Avikainen S, Kirveskari E, Salenius S, Rizzolatti G (1998) *Proc Natl Acad Sci USA* 95:15061–15065.
7. Iacoboni M, Woods R, Brass M, Bekkering H, Mazziota J, Rizzolatti G (1999) *Science* 286:2526–2528.
8. Nishitani N, Hari R (2000) *Proc Natl Acad Sci USA* 97:913–918.
9. Nishitani N, Hari R (2002) *Neuron* 36:1211–1220.
10. Fogassi L, Ferrari P, Gesierich B, Rozzi S, Chersi F, Rizzolatti G (2005) *Science* 308:662–667.
11. Salmelin R, Hari R (1994) *Neuroscience* 60:537–550.
12. Hari R, Salmelin R (1997) *Trends Neurosci* 20:44–49.
13. Chen R, Corwell B, Hallett M (1999) *Exp Brain Res* 129:77–86.
14. Niedermeyer E (2005) in *Electroencephalography: Basic Principles, Clinical Applications and Related Fields*, eds Niedermeyer E, Lopes da Silva F (Lippincott Williams & Wilkins, Philadelphia), pp 167–192.
15. Jensen O, Goel P, Kopell N, Pohja M, Hari R (2005) *NeuroImage* 26:347–355.
16. Kilner J, Baker S, Salenius S, Hari R, Lemon R (2000) *J Neurosci* 20:8839–8845.
17. Mäkelä J, Kirveskari E, Seppä M, Hämäläinen M, Forss N, Avikainen S, Salonen O, Salenius S, Kovala T, Randell T, Jääskeläinen J, Hari R (2001) *Hum Brain Mapp* 12:180–192.
18. Gerloff C, Braun C, Staudt M, Hegner LY, Dichgans J, Krägeloh-Mann I (2006) *Hum Brain Mapp* 27:789–798.
19. Kohler E, Keysers C, Umiltà M, Fogassi L, Gallese V, Rizzolatti G (2002) *Science* 297:846–848.
20. Aziz-Zadeh L, Iacobini M, Zaidel E, Wilson S, Mazziota J (2004) *Eur J Neurosci* 19:2609–2612.
21. Flanagan J, Johansson R (2003) *Nature* 424:769–771.
22. Kilner J, Vargas C, Duval S, Blakemore S, Sirigu A (2004) *Nat Neurosci* 7:1299–1301.
23. Babiloni C, Babiloni F, Carducci F, Cincotti F, Cocozza G, Del Percio C, Moretti DV, Rossini PM (2002) *NeuroImage* 17:559–572.
24. Merleau-Ponty M (1945) *Phénoménologie de la Perception* (Gallimard, Paris).
25. Mead GH (1934) *Mind, Self, and Society from the Standpoint of a Social Behaviorist*, ed Morris CW (Univ of Chicago Press, Chicago).
26. Nishitani N, Avikainen S, Hari R (2004) *Ann Neurol* 55:558–562.
27. Farrer C, Franck N, Frith CD, Decety J, Georgieff N, d'Amato T, Jeannerod M (2004) *Psychiatry Res* 131:31–44.
28. Hari R, Nishitani N (2004) in *Functional Neuroimaging of Visual Cognition. Attention and Performance XX*, eds Kanwisher N, Duncan J (Oxford Univ Press, Oxford), pp 463–479.
29. Ruby P, Decety J (2001) *Nat Neurosci* 4:546–550.
30. MacDonald PA, Paus T (2003) *Cereb Cortex* 13:962–967.
31. Vogeley K, May M, Ritzl A, Falkai P, Zilles K, Fink GR (2004) *J Cognit Neurosci* 16:817–827.
32. Jackson P, Meltzoff A, Decety J (2006) *NeuroImage* 31:429–439.
33. Avikainen S, Forss N, Hari R (2002) *NeuroImage* 15:640–646.
34. Hasson U, Nir Y, Levy I, Fuhrmann G, Malach R (2004) *Science* 303:1634–1640.
35. Möttönen R, Järveläinen J, Sams M, Hari R (2005) *NeuroImage* 24:187–192.
36. Hämäläinen M, Hari R, Ilmoniemi R, Knuutila J, Lounasmaa OV (1993) *Rev Mod Phys* 65:413–497.